Electronic Supplementary Information

A novel nitrogen-doped reduced graphene oxide-bonded Sb nanoparticles for improved sodium storage performance

Yuyan Fang,[a,c] Xin Xu,[a,c] Yichen Du,[a] Xiaoshu Zhu,[b] Xiaosi Zhou*[a] and Jianchun Bao[a]*

[a] Jiangsu Key Laboratory of New Power Batteries, Jiangsu Collaborative Innovation Center of Biomedical Functional Materials, School of Chemistry and Materials Science, Nanjing Normal University, Nanjing 210023, China

[b] Center for Analysis and Testing, Nanjing Normal University, Nanjing 210023, China

[c] Y.F. and X.X. contributed equally to this work.

*Corresponding authors. E-mail: zhouxiaosi@njnu.edu.cn; xiaoshu_zhu78@163.com

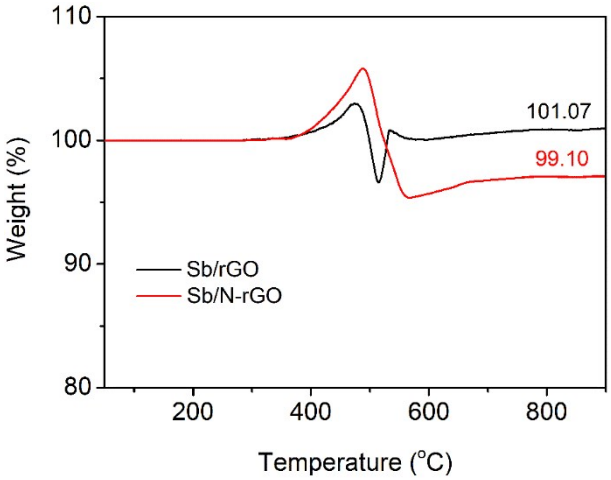

Fig. S1 TGA curves of Sb/N-rGO and Sb/rGO in air with a heating rate of 10 ℃ min^{-1} from room temperature to 900 ℃. The weight fractions of Sb in the Sb/N-rGO and Sb/rGO composites can be determined based on the weight loss from carbon combustion and the weight gain from the formation of Sb_2O_4. According to the following Equation S1, the contents of Sb in Sb/N-rGO and Sb/rGO are calculated to be about 78.5 and 80.1 wt%, respectively.

$$\text{Sb (wt\%)} = \frac{2 \times \text{atomic weight of Sb}}{\text{molecular weight of } Sb_2O_4} \times \frac{\text{final weight of } Sb_2O_4}{\text{initial weight of Sb/C}}$$

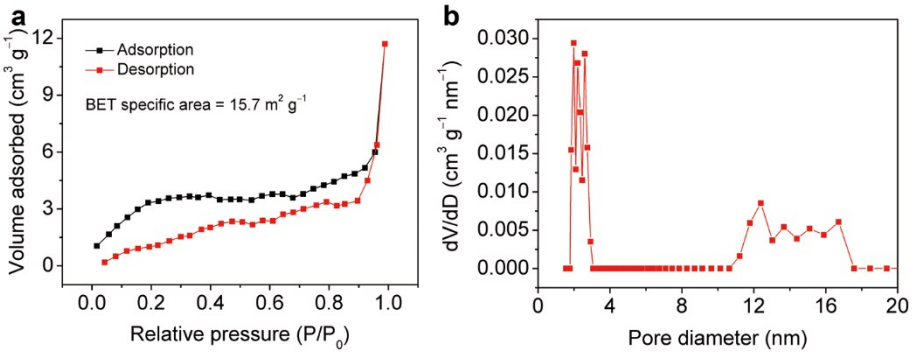

Fig. S2 (a) N_2 adsorption/desorption isotherms and (b) corresponding pore size distribution of Sb/N-rGO.

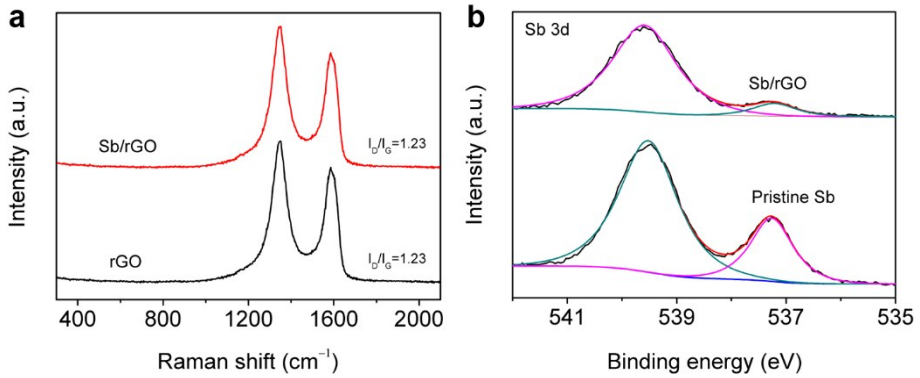

Fig. S3 (a) Raman spectra of Sb/rGO and rGO. (b) High-resolution Sb 3d XPS spectra of Sb/rGO and pristine Sb.

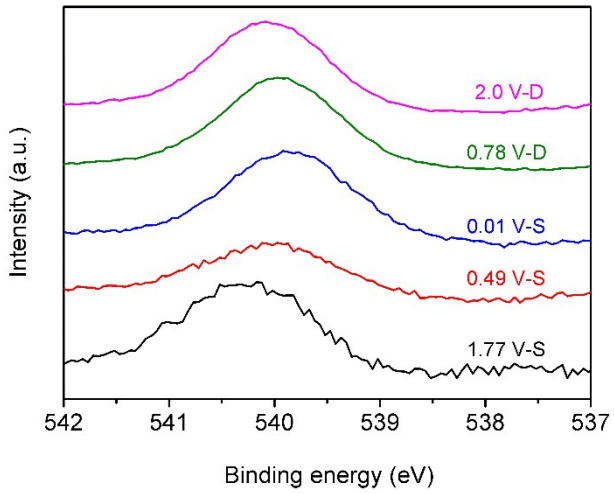

Fig. S4 Ex situ Sb 3d XPS curves of the Sb/N-rGO electrode at different stages of sodiation (S) and desodiation (D).

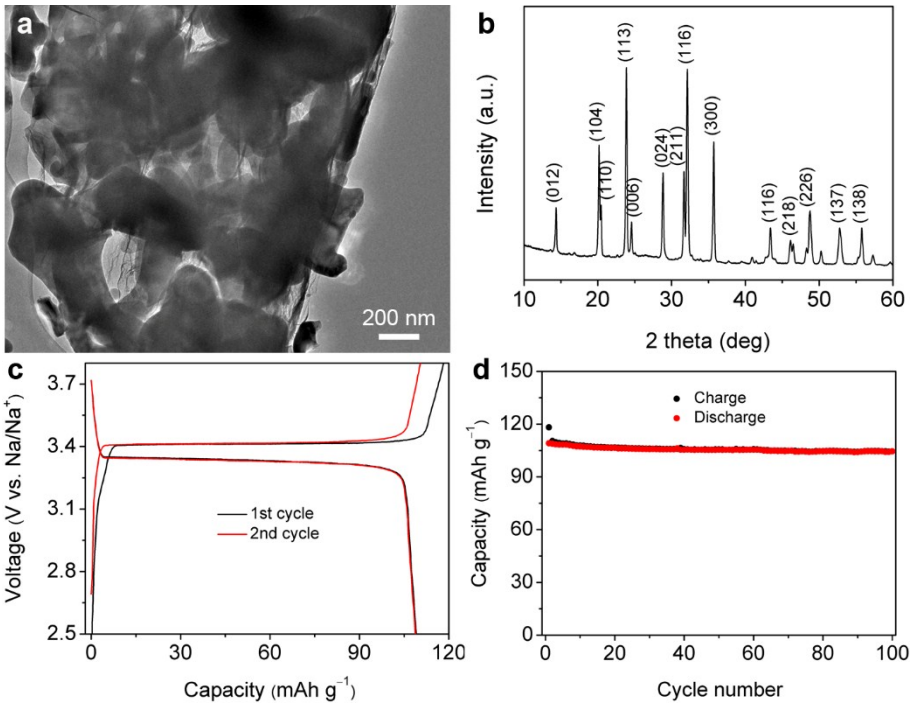

Fig. S5 (a) TEM image, (b) XRD pattern, (c) charge−discharge profiles, and (d) cycling performance of the $Na_3V_2(PO_4)_3$/C cathode between 2.5 and 3.8 V at 1 C (1 C = 118 mA g^{-1}).

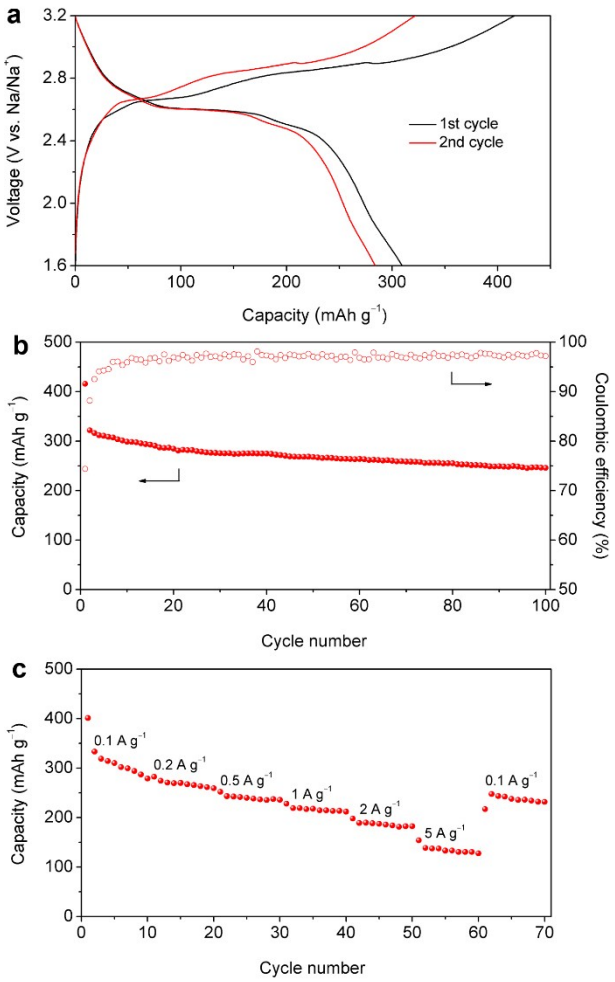

Fig. S6 (a) Charge−discharge voltage curves of the full cell consisting of Sb/N-rGO anode and $Na_3V_2(PO_4)_3$/C cathode at 0.1 A g^{-1}. (b) Cycling performance and corresponding Coulombic efficiency of the full cell at 0.1 A g^{-1}. (c) Rate capability of the full cell.

Table S1 Comparison of sodium storage properties of various Sb-based anode materials.

Sb-based anode materials	Reversible capacity (mAh g^{-1})	Cycling stability	Rate capability (mAh g^{-1})	Ref.
Sb/N-rGO	521.9 (100 mA g^{-1})	90.7% (500 cycles)	304.8 (5 A g^{-1})	This work
Sb-NDs⊂CNs	507 (100 mA g^{-1})	94% (100 cycles)	271 (2 A g^{-1})	1
Sb@NC	440 (100 mA g^{-1})	75% (300 cycles)	237 (5 A g^{-1})	2
hollow Sb@C yolk−shell spheres	600 (50 mA g^{-1})	82% (100 cycles)	279 (4.2 A g^{-1})	3
Sb@C-5	473 (100 mA g^{-1})	86% (240 cycles)	370 (5 A g^{-1})	4
Sb@TiO_{2-x}	549 (2.64 A g^{-1})	55% (1000 cycles)	312 (13.2 A g^{-1})	5
Sb/MLG	452 (100 mA g^{-1})	90% (200 cycles)	210 (5 A g^{-1})	6
10-Sb@C	435 (100 mA g^{-1})	88.5% (500 cycles)	270 (4 A g^{-1})	7
Sb-N/C	796 (50 mA g^{-1})	38.3% (60 cycles)	142 (10 A g^{-1})	8
Sb−C nanofibers	495 (200 mA g^{-1})	90% (400 cycles)	337 (3 A g^{-1})	9
SbNP@C	422 (100 mA g^{-1})	82.9% (300 cycles)	104 (5A g^{-1})	10
SbNP/MWCNT	502 (200 mA g^{-1})	76% (120 cycles)	225 (2 A g^{-1})	11
Sb/C	610 (100 mA g^{-1})	94% (100 cycles)	309 (2 A g^{-1})	12

Table S2 Kinetic parameters of the electrodes.

Samples	R_{SEI} (Ω)	R_{ct} (Ω)
Sb/N-rGO	21.7	99.0
Sb/rGO	33.3	155.9
Sb	41.5	202.3

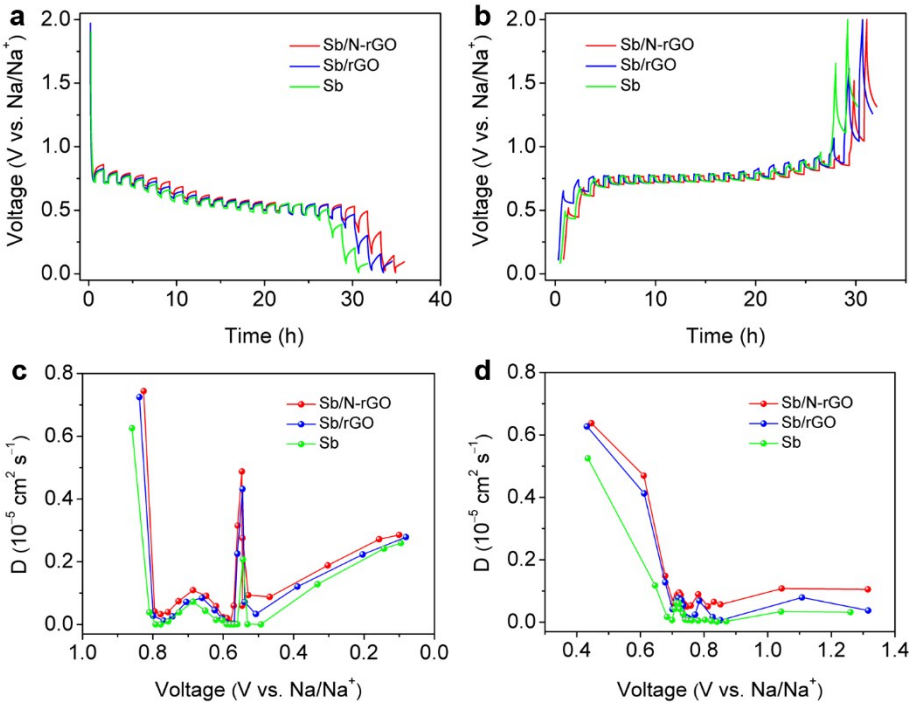

Fig. S7 GITT curves of Sb, Sb/rGO, and Sb/N-rGO for (a) sodiation and (b) desodiation of the second cycle. Corresponding sodium ion apparent diffusion coefficients of Sb, Sb/rGO, and Sb/N-rGO for (c) sodiation and (d) desodiation.

According to the Fick's second law of diffusion, the diffusivity coefficient of sodium ions (D_{Na^+}) can be calculated based on the following equation:[13]

$$D_{Na^+} = \frac{4}{\pi\tau}\left(\frac{m_B V_M}{M_B S}\right)^2 \left(\frac{\Delta E_s}{\Delta E_t}\right)^2$$

where τ is the pulse duration, m_B is the mass of active material, M_B is the molar mass of Sb, V_M is the molar volume, and S is the active surface area of the Sb/N-rGO electrode. ΔE_s and ΔE_t can be gotten from the GITT curves (Fig. S7a and b). As shown in Fig. S7c and d, sodium ion diffusivity coefficient attains a magnitude of 10^{-6} cm^2 s^{-1}.

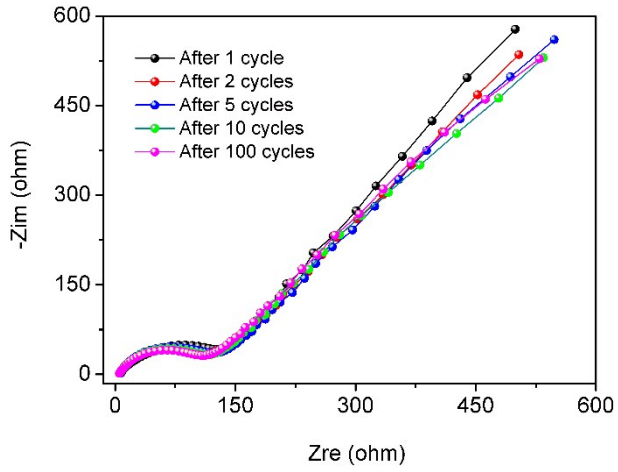

Fig. S8 Nyquist plots of the Sb/N-rGO electrode after different cycles.

Table S3 Kinetic parameters of the Sb/N-rGO electrode after various cycles.

Samples	R_{SEI} (Ω)	R_{ct} (Ω)
After 1 cycle	21.7	99.0
After 2 cycles	20.2	97.4
After 5 cycles	19.3	96.5
After 10 cycles	18.7	95.8
After 100 cycles	18.4	94.9

References

1. C. Wu, L. F. Shen, S. Q. Chen, Y. Jiang, P. Kopold, P. A. van Aken, J. Maier and Y. Yu, *Energy Storage Mater.*, 2018, **10**, 122.
2. X. Xu, Z. Dou, E. Gu, L. Si, X. Zhou and J. Bao, *J. Mater. Chem. A*, 2017, **5**, 13411.
3. J. Liu, L. Yu, C. Wu, Y. Wen, K. Yin, F. K. Chiang, R. Hu, J. Liu, L. Sun and L. Gu, *Nano Lett.*, 2017, **17**, 2034.
4. Z. M. Liu, X. Y. Yu, X. W. D. Lou and U. Paik, *Energy Environ. Sci.*, 2016, **9**, 2314.
5. N. Wang, Z. Bai, Y. Qian and J. Yang, *Adv. Mater.*, 2016, **28**, 4126.

6. L. Hu, X. Zhu, Y. Du, Y. Li, X. Zhou and J. Bao, *Chem. Mater.*, 2015, **27**, 8138.
7. N. Zhang, Y. Liu, Y. Lu, X. Han, F. Cheng and J. Chen, *Nano Res.*, 2015, **8**, 3384.
8. X. Zhou, Y. Zhong, M. Yang, M. Hu, J. Wei and Z. Zhou, *Chem. Commun.*, 2014, **50**, 12888.
9. L. Wu, X. Hu, J. Qian, F. Pei, F. Wu, R. Mao, X. Ai, H. Yang and Y. Cao, *Energy Environ. Sci.*, 2014, **7**, 323.
10. Y. Zhu, X. Han, Y. Xu, Y. Liu, S. Zheng, K. Xu, L. Hu and C. Wang, *Acs Nano*, 2013, **7**, 6378.
11. X. Zhou, Z. Dai, J. Bao and Y. G. Guo, *J. Mater. Chem. A*, 2013, **1**, 13727.
12. J. Qian, Y. Chen, L. Wu, Y. Cao, X. Ai and H. Yang, *Chem. Commun.*, 2012, **48**, 7070.
13. W. Weppner and R. A. Huggins, *J. Electrochem. Soc.*, 1977, **124**, 1569.